J. Membrane Biol. 130, 241–249 (1992)

The Journal of
Membrane Biology

Anion and Cation Permeability of a Large Conductance Anion Channel in the T84 Human Colonic Cell Line

Luis Vaca and Diana L. Kunze
Department of Molecular Physiology and Biophysics, Baylor College of Medicine, Houston, Texas 77030

Summary. A large conductance multi-state channel was identified and characterized in single channel recordings from cell-attached and excised patches of the human colonic tumor cell line, T84. The channel activity was dependent on the presence of both permeable cations and anions. In Na^+-free symmetrical Cl^- solutions or Cl^--free symmetrical Na^+ solutions the channel was inactive. Addition of 5 mM NaCl (NaI or KCl) induced channel activity. The selectivity sequence obtained from the shift in reversal potential was $I^-(1.9) > Cl^-(1) > Na^+(0.5) > K^+(0.3)$. SO_4^{2-}, SCN^- (thiocyanate) and $NMDG^+$ were impermeant. Multiple subconductance states were identified at all voltages explored (±90 mV). The minimum conductance encountered in symmetrical 100 mM NaCl was a 15 pS substate, the maximum, 210 pS. The channel appeared to be composed of multiples of the 15 pS subunits which were reversibly blocked by the loop diuretic bumetanide (5 μM).

Key Words patch clamp · subconductance states · chloride channel · anion-cation permeability · bumetanide

Introduction

An agonist-induced Cl^- pathway has been previously described in the human colonic cell line T84 [14]. Another important pathway for Cl^- conduction in this cell line appears to be a volume-activated Cl^- conductance [23]. In an attempt to explore alternative pathways for Cl^- and Na^+ conduction, we have examined single channel activity in the T84 cells using the patch-clamp technique.

In the present study we have identified another pathway for Cl^- and Na^+ movement, a large conductance poorly selective anion channel. This channel has some of the characteristics of high conductance voltage-gated anion channels (HVACs) described in other epithelial cells such as renal A6 cells [15], bovine kidney cells (GBK) [22], sweat gland epithelia [12] and pulmonary alveolar cells [18]. These characteristics include multiple substates, conductance larger than 200 pS, low channel activity in cell-attached patches and activation by strong depolarization. However, the channel described here is unique because the open state is dependent on the simultaneous presence of both permeable cations and anions. In this regard it resembles a Na^+-dependent Cl^--selective channel found in hippocampal neurons [5].

Material and Methods

Cell Culture

The T84 cell line was purchased from American Type Culture Collection as frozen cells in passage number 59. Cells were prepared in one of two ways: (a) plated on culture dishes previously coated with collagen (Sigma IV) or (b) plated on permeable filters millicell-CM (Millipore) also coated with collagen (Sigma). The cells were grown in Dulbecco's modified medium supplemented with 10% fetal bovine serum with 1% streptomycin, penicillin and neomycin at 37°C in an atmosphere of 5% CO_2. Confluency was reached in approximately one week. Cells were used from passage 60 to 90.

Cells were prepared for cell-attached, inside-out and outside-out patch clamp experiments in one of two ways. Either the media were replaced with the solution to be used in the experiment and the cells studied directly, or the media were removed and the cells treated for 2 min at room temperature with Hank's basic salt solution containing 0.25% trypsin. The second treatment improved the number of successful patches, possibly by removing secretory material from the surface of the monolayer which may interfere with the patch pipette. After treatment, trypsin solution was replaced by the extracellular solution. The two methods of preparation gave similar results regarding ion selectivity and voltage sensitivity.

Solutions

All the salts used were analytical grade (Sigma). Osmolarity of all solutions was adjusted to 300 mM with sucrose. The NaCl-l solution contained 50 mM NaCl and the NaCl-h solution contained 100 mM NaCl. Other solutions used contained in mM: 100

NMDGC1, 100 Na_2SO_4, 100 NaI, 100 KCl, 100 NaSCN. The extracellular solution used in cell-attached experiments contained in mM: 145 NaCl, 5 KCl, 1 $CaCl_2$, 1 $MgCl_2$. All the solutions were buffered with 10 mM Tris (hydroxymethyl) amino methane and adjusted to pH 7.2, with either HCl or H_2SO_4. The calcium concentration in all the solutions was maintained at 1 μM with ethyleneglycol-bis-(β-aminoethyl ether)-N,N,N',N'-tetraacetic acid (EGTA) (Sigma), according to the calculations of Fabiato [3]. The perfusion system was designed to allow replacement of the bath solution in less than 1 min.

Channel Blockers

Bumetanide (Sigma) was dissolved in dimethylsulfoxide (DMSO) and diluted to a final DMSO concentration of 1%. This concentration of DMSO alone was tested without effect on the channel. 4,4'-diisothiocyanatostilbene-2,2'-disulfonic acid (DIDS) and 4-acetamido-4'-isothiocyanatostilbene-2,2'-disulfonic acid (SITS) (Sigma) were diluted directly in the NaCl-h solution.

Phosphorylating Cocktail

The phosphorylating cocktail used in inside-out patches contained 450 nM of the catalytic subunit of the cAMP-dependent protein kinase (Sigma), 1 mM of 5'-adenosine triphosphate (ATP-Mg^{2+}). The catalytic subunit was diluted in the buffer to be used and 1 mg of dithiotreitol (DTT) was added to the solution. The mixture was incubated for 10 min at room temperature prior to use. The catalytic subunit was prepared fresh for each set of experiments.

Patch Clamp

Data was obtained using the Axopatch amplifier 1C (Axon Instruments). All experiments were recorded on FM tape. The patch-clamp technique as described by Hamill et al. [9] was used in the cell-attached, inside-out and outside-out configurations to study confluent T84 monolayers. The resistance of the pipettes (7052 or 8161 glass, Garner) filled with 100 mM NaCl was 5–10 mΩ. All patch experiments were performed at 37°C. Selected data were filtered to 5 KHz with an 8-pole Bessel filter (Frequency Devices) and digitized for computer analysis. In most of the experiments both the pipette and the initial bathing solution were 100 mM NaCl. The zero current was obtained with the electrode in the bath prior to formation of the cell-attached patch. Changes in the liquid junction potential at the reference electrode that occurred when the bath solution was changed during the selectivity experiments were minimized by the use of a 150 mM KCl agar bridge as the reference electrode. These potentials were estimated during localized perfusion of the open tip of the agar bridge and ranged from 1 to 4 mV. In experiments in the outside-out patch configuration no corrections were attempted as these experiments were designed only to demonstrate the effect of bumetanide on channel activity.

Single Channel Analysis

Fetchex (Axon Instruments) was used to digitize channel activity at a sampling rate of 100 μsec/point (10 kHz). Fetchan (Axon Instruments) was used for single channel analysis. This program is based on the half amplitude criteria. The appearance of multiple levels produced a large variability in current amplitude among experiments. The channel amplitude used to calculate channel conductance was obtained as follows. Three to five minutes after channel activity was initiated the channel attained a relatively stable maximum amplitude. Total point amplitude histograms were then obtained during, at least, one minute of continuous recording and binned at 0.2 pA. The histogram obtained under these conditions was fitted with a Gaussian function and the mean value obtained from the largest peak in the histogram was selected. This procedure was repeated for all the holding potentials reported in the experiments. Channel open probability (*Po*) was measured after channel activity reached a stable amplitude. To calculate channel *Po*, we used only events higher than half the amplitude of the fully open state (half-amplitude criteria). The time used to calculate channel *Po* is indicated in the figure legends.

Selected traces of single channel activity were obtained from the binary file and transformed to HPGL (Hewlett-Packard graphic language) files for illustrative purposes. Total events histograms were generated from Fetchan files with Sigmaplot 4.0 (Jandel) and plotted as above. Data is presented with the mean ± SD.

Results

Cell-Attached Patches

The channel that is the subject of this report was initially studied in the cell-attached configuration. It was present with a low probability of opening (<10 events/sec) in approximately 30% of the patches explored in the cell-attached configuration (34/145) with no potential applied to the patch (cell resting potential). Its identity was verified upon excising the patch to the inside-out configuration based on the following criteria: (i) presence of multiple subconductance states; (ii) no change in conductance upon excision and (iii) reversal potential near 0 mV with asymmetrical NaCl. With NaCl-h (100 mM NaCl) in the pipette and in the bath the channel reversal potential (E_{rev}) obtained in cell-attached mode occurred at an applied patch potential of -26.5 ± 5.3 mV ($n = 10$).

Exposing the cells (in cell-attached mode) to 1 mM of the permeable derivative dibutyryl-cAMP produced variable results regarding channel activation. Channel activity appeared within 2 min in only 20% of the patches subsequently confirmed to contain this channel (6/30). Two substances that increase intracellular cAMP levels in T84 cells [14] were also examined for their ability to induce channel activity in quiescent patches. Activity appeared in only 5/35 cell-attached patches after 50–100 μM isoproterenol was applied. Vasoactive intestinal peptide (VIP) was equally ineffective; channel activity appeared in only 4/20 patches in response to 0.1–1.0 μM VIP.

Application of strong polarizing pulses to the

patch, more positive than +50 mV or more negative than −50 mV, induced channel activity in 50% of the cell-attached patches tested (10/20). However, this channel activity returned to control values 2–3 minutes following polarization (returning to the resting potential).

Inside-Out Patches

In 70% of the cell-attached patches channel activity was not present (111/145). These patches of membrane without channel activity were excised from the cell and a potential outside the range of ±50 mV was applied to the patch. Channel activity appeared within 3 min in 65 of the 111 patches that had no previous activity in the cell-attached mode.

In the following experiments patches were routinely excised to the inside-out configuration immediately after seal formation (n = 420). The membrane potential was held outside the range of ±50 mV and activation of the channel was usually initiated within 3 min. It appeared first as an instability of the baseline resembling a "leaky patch." Within a few seconds baseline stability recovered and channel activity was initiated as a small conductance which increased in multiple amplitude steps to a final maximum amplitude within 3–5 min. Figure 1 shows an example of such activity. Transitions among various sublevels continued and the closed state could be reached from any of several levels. There was a large variability in maximum amplitude among experiments. However, it was possible to identify a minimum amplitude which was present in the majority of our patches. This minimum amplitude which can be observed at the beginning of the first record in Fig. 1 was seen in all the patches before appearance of supralevels. The maximal amplitude observed appeared to be composed of aggregates of the minimum amplitude.

Figure 2*A* shows the current-voltage relationship for the minimum amplitude level obtained from a patch in which it was possible to explore several voltages before the appearance of additional levels. The smallest conductance level observed under symmetrical NaCl-h conditions (Fig. 2*B*) was approximately 15 ± 2 pS (n = 10). All the levels were considered as part of the same channel based on the following criteria: (i) all amplitudes reversed at the same potential in ion replacement experiments, (ii) all amplitudes were reversible blocked by bumetanide and (iii) baseline could be reached from any level. Multiple conductance levels were observed at all the voltages explored (±90 mV). The mean of the largest conductance level in 130 patches in symmetrical NaCl-h was 210 pS (±20 pS), which corresponds to 14–15 aggregates of the 15 pS subconductance states.

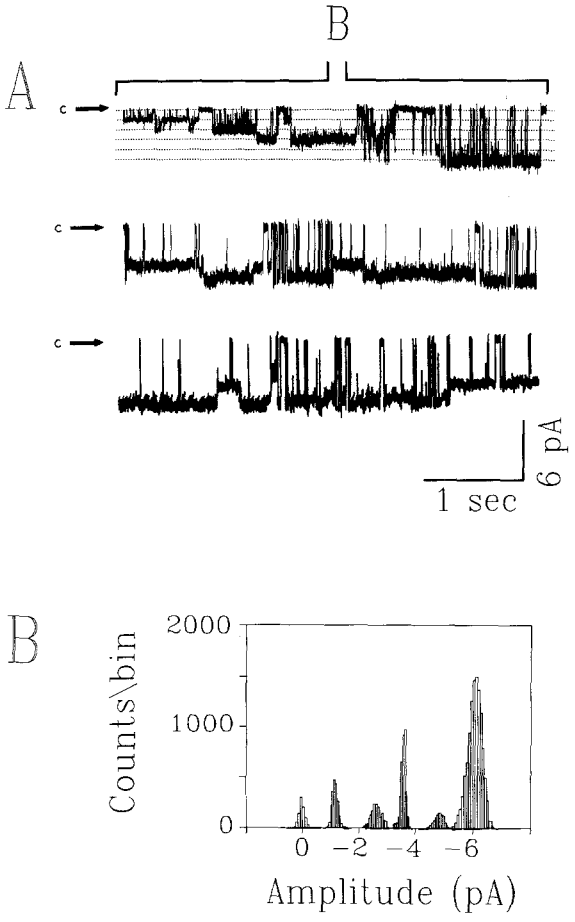

Fig. 1. *Panel A*. Consecutive records of channel activity in an inside-out patch. Channel was activated by holding the membrane potential at −60 mV for 3 min. Channel activity was initiated as a small amplitude followed by fast transitions to various levels with higher amplitudes. The maximum amplitude was composed of six equally-sized subconductance states, corresponding roughly to zero current (base line), 1.2 pA, 2.4 pA, 3.5 pA, 4.8 and 6 pA. Each amplitude level increment was about 1.2 pA which corresponds to the amplitude of the smallest subconductance state at this holding (*see* Fig. 2). The closed level (indicated by the arrows) could be reached several times within a second, from any of the amplitude levels, which would be unlikely in a patch with multiple independent channels. *Panel B*. Total points amplitude histograms obtained from the first trace in *A*. The six peaks correspond to the six levels indicated by the dotted lines in *Panel A*. The voltage is reported with the extracellular solution as reference (for inside-out patch the pipette is the reference). Channel activity was low pass filtered at 5 kHz and digitized at 10 kHz. The solution is NaCl-h (100 mM NaCl) in both sides of the membrane, the holding potential is −60 mV.

Phosphorylating Cocktail

In a separate set of 56 excised patches that showed no activity prior to excision the patch potential was

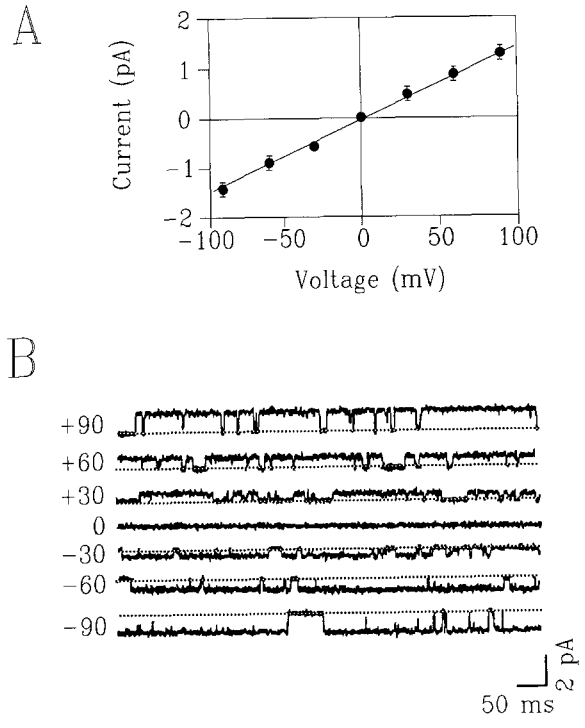

Fig. 2. Example of activity from an inside-out patch containing the smallest subconductance state displayed by the channel in symmetrical NaCl-h (100 mM NaCl). *Panel A* shows the current-voltage relationship obtained from 10 different experiments and *Panel B* shows traces with channel activity at the holding potentials indicated to the left of each record. The channel conductance obtained under these experimental conditions was 15 ± 2 pS (n = 10). The solid line drawn through the points in *Panel A* represents a linear least-squares fit. Closed level is indicated by the dotted lines. Channel activity was low pass filtered at 1 kHz and digitized at 5 kHz.

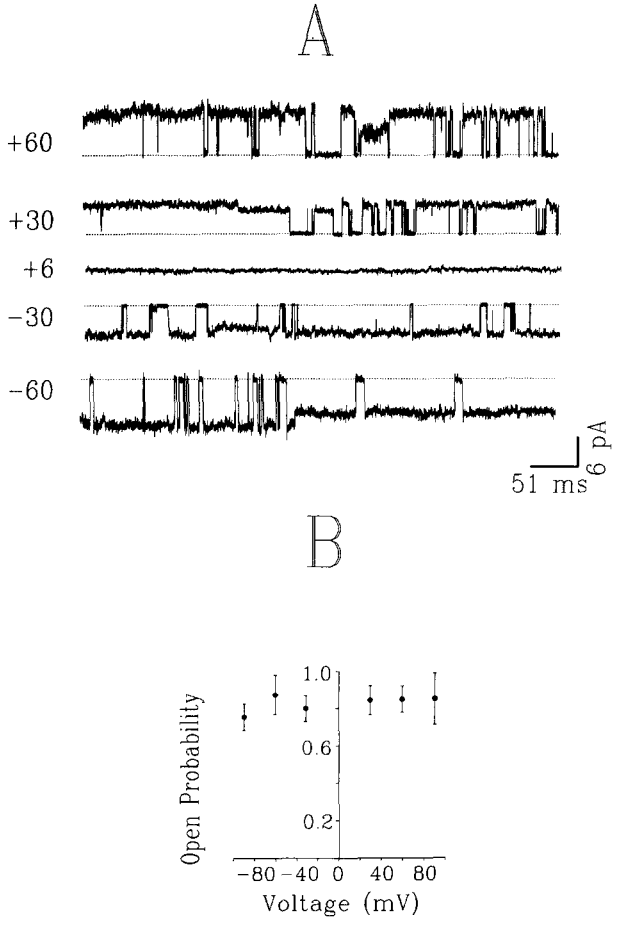

Fig. 3. *Panel A.* Activity of an inside-out patch in asymmetrical NaCl. The pipette solution contained NaCl-1 (50 mM NaCl) and the bath solution NaCl-h (100 mM NaCl). All the conductance levels reversed direction at +6.0 mV. Under these conditions E_{Cl^-} should be +18.0 mV and E_{Na^+}, −18.0 mV. Closed level is indicated by the dotted lines. The numbers shown at the left of the traces indicate the holding potential with the pipette (extracellular) solution as reference. The channel conductance (166 pS) was calculated from the largest amplitude peak obtained with a multiple Gaussian fit of the total points amplitude histograms at each holding potential. This channel conductance (166 pS) corresponds to approximately 11 of the 15 pS subunits. *Panel B.* Open probability (*Po*)-voltage curve. As indicated in the figure, the channel showed no voltage sensitivity in the range explored (±90 mV). Channel *Po* was obtained from 1-min records at each voltage. The half amplitude criteria was used to separate the open from the closed level. Channel events larger than the half amplitude of the fully open state were considered as an opening event. Channel activity was low pass filtered at 5 kHz and digitized at 10 kHz.

held within the range of ±20 mV (usually +10 mV) to reduce the possibility of activation by voltage. The effect of a phosphorylating cocktail was tested by application to the intracellular surface. Channel activity was observed within 2 min after addition of the phosphorylating cocktail in only 10 of the 56 patches explored. To demonstrate that channels were present in the unresponsive patches (46/56), depolarization or hyperpolarization beyond ±50 mV was applied. Channel activity in 32 of the 46 patches occurred within 5 min of polarization.

Ion Selectivity

To determine which ion permeates the channel, we designed experiments to examine the channel selectivity in inside-out patches. With symmetrical NaCl-h solution E_{rev} obtained from 13 different experiments was 0 ± 1 mV.

In another set of experiments, a NaCl gradient using NaCl-1 (50 mM NaCl) as the pipette solution and NaCl-h (100 mM NaCl) in the bath was imposed to determine the selectivity ratio, P_{Na}/P_{Cl}. Figure 3*A* illustrates an example under these experimental

Table. Selectivity ratios for anions and cations

Solutions ([o]/[i])	E_{rev}/mV ± SD	N	P(ion)/P(Cl^-)[a]
NaCl-h/NaCl-h	0 ± 1	13	—
NaCl-l/NaCl-h	6 ± 1.5	35	0.5 ± 0.05 (Na)
NaCl-h/KCl	6 ± 2	26	0.3 ± 0.1 (K)
NaCl-h/NaI	12 ± 2	14	1.9 ± 0.2 (I)
NaCl-h/NMDGCl	5 ± 3.3	42	<0.15 (NMDG)
NaCl-h/NaSCN	−28 ± 5	5	<0.01 (SCN)
NaCl-h/Na_2SO_4	−34 ± 1	4	<0.01 (SO_4)

[a] P[Cl] = 1. [o] = extracellular (pipette for inside-out). [i] = intracellular (bath). E_{rev} = reversal potential (in mV). SD = standard deviation. N = number of patches explored. NaCl-l = 50 mM NaCl. NaCl-h = 100 mM NaCl.

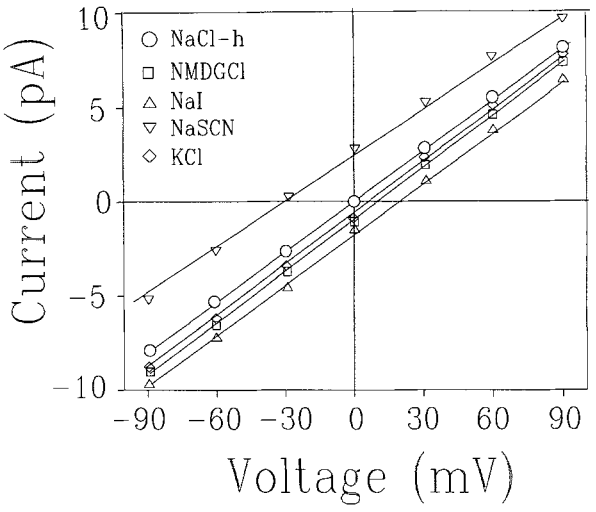

Fig. 4. Effect of ionic composition of the bathing solution on the reversal potential of the multiple conductance channel in an inside-out patch. The pipette solution is NaCl-h, the bath solution was NaCl-h (○), NMDGCl (□), NaI (△), KCl (◇) and NaSCN (▽). To plot the current-voltage relationship, the largest amplitude at each holding potential was obtained from the total points amplitude histograms as in Fig. 3 (*see* Materials and Methods). The solid lines drawn through the data points represent a linear least square fit. Experiments such as this were used to obtain the selectivity ratios shown in the Table.

conditions. All the subconductance states reversed direction of current flow at E_{rev} = 6 ± 1.5 mV (n = 35). As indicated in Fig. 3*B*, this channel is not voltage-gated, since channel *Po* was not affected by changing the membrane potential in the range ±90 mV. Under these ionic conditions E_{rev} calculated for a cation channel should be approximately −18 mV and for an anion channel, +18 mV. A selectivity ratio of P_{Na}/P_{Cl} = 0.5 was obtained from the reversal potential. Similar intracellular ion replacements were performed to determine selectivity ratios for other anions and cations. In these experiments NaCl-h was used in the pipette as test solution while different solutions containing the anion or cation to be tested replaced the intracellular (bath) solution. Assuming a constant permeability ratio of P_{Na}/P_{Cl} = 0.5, the E_{rev} obtained after each ion replacement was used in the Goldman-Hodgkin-Katz equation to calculate selectivity ratios for other cations and anions. The results are summarized in the Table. The current-voltage relationships for a single inside-out patch after replacing the intracellular solution with different cation and anion combinations is shown in Fig. 4.

The results obtained from the selectivity experiments (Table) indicate that this channel differentiates poorly among small anions and cations showing a permeability sequence of $I^-(1.9) > Cl^-(1) > Na^+(0.5) > K^+(0.3)$. SO_4^{-2}, $NMDG^-$ and SCN^- (thiocyanate) were impermeant.

Anion and Cation-Dependent Permeation

While performing ion replacements we observed that in Na^+-free Cl^- solutions or Cl^--free Na^+ solutions channel activity was abolished. In experiments where both the intracellular and extracellular solutions were NMDGCl (n = 31) no current was observed (Fig. 5*A*, left panel). Thus, under these conditions it appeared that Cl^- did not permeate the channel, contrary to what we expected from the selectivity experiments. However, when 5 mM NaCl was added to the bath solution both inward and outward current appeared (Fig. 5*A*). The E_{rev} obtained was 0 ± 3 mV (n = 25). After return to the original bath solution (NMDGCl), the current disappeared (Fig. 5*A*, right panel). In a different set of experiments, with Na_2SO_4 replacing NaCl as the pipette and bath solution, no current was present even though Na^+ was present on both sides of the membrane, as shown in the left panel of Fig. 5*B*. Again, adding 5 mM NaCl to the intracellular surface of the patch elicited current (n = 15) with E_{rev} = 0 ± 2 mV (Fig. 5*B*, center panel). Replacing the bath solution with Na_2SO_4 without Cl^- abolished the current (Fig. 5*B*, right panel).

Since K^+ is another cation that permeates the channel, we tested the effect of adding 5 mM KCl instead of NaCl in a set of experiments similar to those described above (with symmetrical Na_2SO_4). The time course of activation induced by NaCl and KCl are shown in Fig. 6. As shown in Fig. 6*A* and *B*, both (NaCl or KCl) were effective in activating the channel. Replacing 5 mM KCl for 5 mM NaCl induced a shift in E_{rev} of 2 mV ± 1.2 mV (n = 8) as expected according to the difference in selectivity ratios for Na^+ and K^+ (*see* Table). Channel activa-

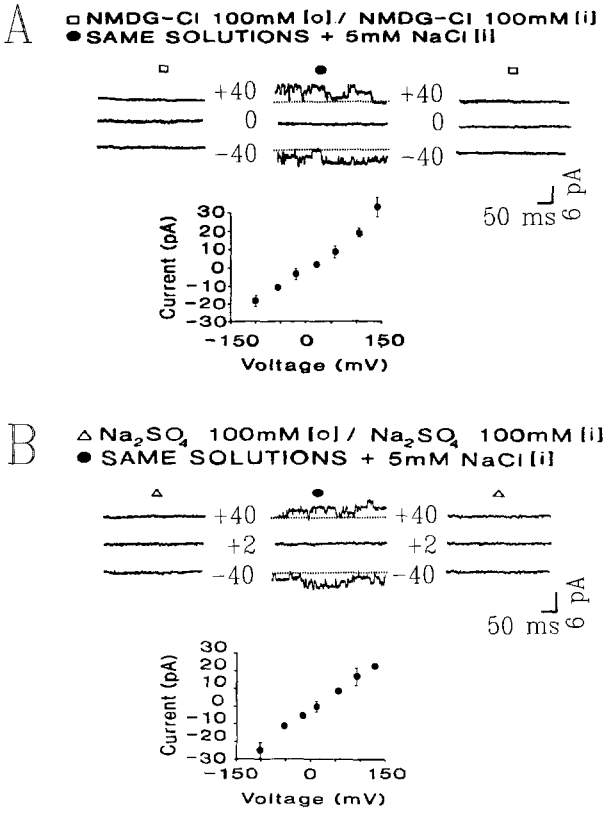

Fig. 5. *Panel A.* The control experiment on the left panel (□) in symmetrical NMDGCl shows no current after exploring several holding potentials (only three are shown). Addition of 5 mM NaCl to the bath (intracellular) solution as shown in the middle panel (●) evoked channel activity with a E_{rev} = 0 mV. In the right panel channel activity disappeared after removing the NaCl from the bath (□). Below the panel the current-voltage relationship is shown for the different voltages explored (n = 17). *Panel B.* A similar sequence to the above was performed in another patch with pipette and bath solutions of Na_2SO_4 (△) illustrated in the left panel. Again after addition to 5 mM NaCl (●) channel activity was evoked (central panel). Removing NaCl from the bath abolished the current (△) as shown in right panel. Below the sequence is shown the current-voltage relationship for 15 different patches. Channel activity was low pass filtered at 5 kHz and digitized at 10 kHz. The channel amplitude used to produce the current-voltage relationships was obtained from the maximum level of total points amplitude histograms for each holding potential as indicated in Fig. 3.

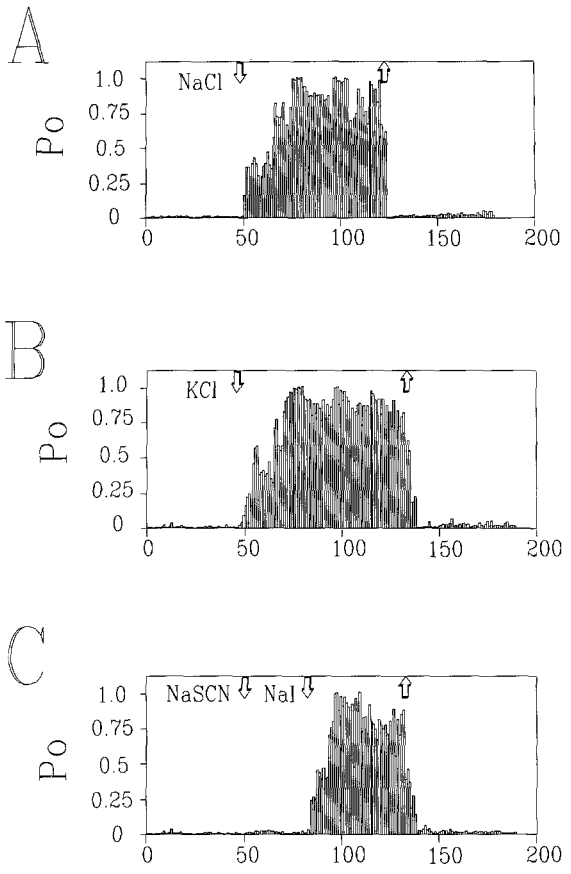

Fig. 6. *Panel A.* Time course of the single channel open probability (*Po*) induced by addition of 5 mM NaCl to an inside-out patch previously maintained in symmetrical Na_2SO_4. Under symmetrical Na_2SO_4 no channel activity was observed; however, immediately after addition of 5 mM NaCl (*downward arrow*) channel activity was initiated with a E_{rev} of 0 mV (*not shown*). After returning the bath solution to Cl^--free Na_2SO_4 solution, channel activity disappeared. *Panel B.* Same patch as in *A*, in this case 5 mM KCl was used instead of NaCl. *Panel C.* Same patch as in *A* and *B*. Channel activity was monitored with symmetrical Na_2SO_4 solutions and after addition of 5 mM NaSCN. NaSCN failed to induce channel activity; however, addition of 5 mM NaI activated the channel. Removing NaI from the bath restored the original conditions. *Po* was calculated every second as indicated in Materials and Methods. The holding potential was +60 mV (pipette as reference).

tion induced by the NaCl or KCl was observed within seconds after addition of the solution to the bath. In the next set of experiments the effect of replacing the anion was assessed. Symmetrical NaSCN failed to activate the channel as expected since SCN^- is impermeable. However, 5 mM NaI induced channel activity with a similar time course activation as that produced by NaCl or KCl (Fig. 6*C*). These results indicate that the combination of a permeable cation and a permeable anion is needed to permit channel activity.

Channel Blockers

Figure 7 represents one example from a set of 40 experiments in which several concentrations of the loop diuretic bumetanide were used in outside-out patches. In these experiments channel activity was monitored under the control conditions and after bumetanide was added to the bath to a final concentration of 5 μM. The full concentration-response range was not tested. However, 10 μM bumetanide produced complete block in all cases (n = 10). Bu-

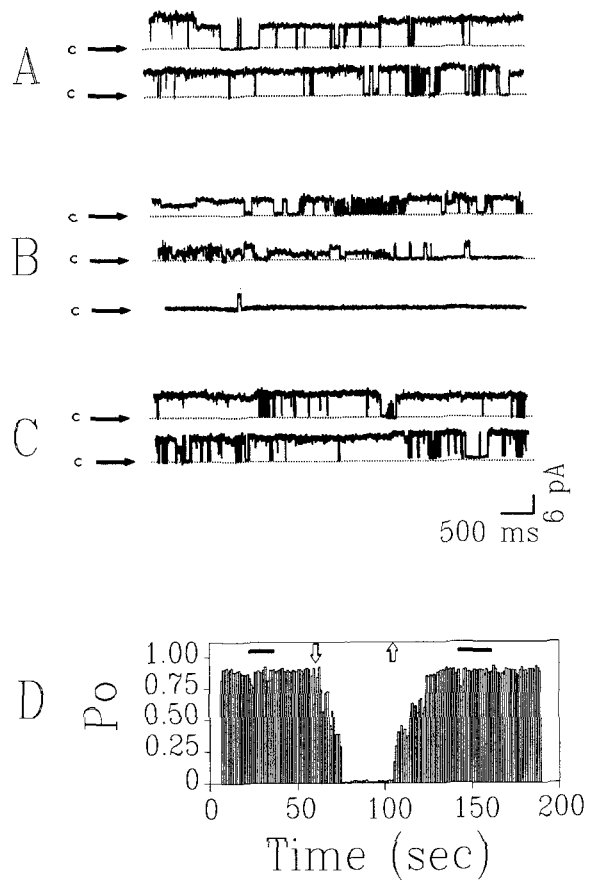

Fig. 7. *Panel A.* An example of activity from an outside-out patch containing the multiple conductance channel. Channel activity was monitored for 10 min before adding bumetanide (10 sec are shown). *Panel B.* The same patch as in *A* showing the effect of bumetanide 40 sec after the bath solution was replaced completely for NaCl-h and 5 μM bumetanide in DMSO (final DMSO concentration 1%). Current amplitude was reduced and there was an increase in the number of transitions to subconductance levels. *Panel C.* The same patch, one minute after removing bumetanide from the bath channel activity recovered to control values. *Panel D.* Time course of blockage induced by bumetanide. Channel open probability was calculated every second. The solid line indicates the point where 1% DMSO was added to the bath solution (solid line). As shown, DMSO produced no effect on channel activity. After removing DMSO, 5 μM bumetanide was added in 1% DMSO (*downward arrow*) channel activity was affected almost immediately. Removing bumetanide and DMSO from the bath produced a full recovery of channel activity (*upward arrow*). Re-addition of 1% DMSO had no effect on channel activity (solid line). Channel activity was filtered at 5 kHz and digitized at 10 kHz. The holding potential throughout the experiment is +60 mV (bath as reference).

metanide affected the channel in two different ways. First, the open probability was reduced from 0.89 ± 0.12 in control conditions to 0.03 ± 0.06 after about 20 sec in the presence of 5 μM bumetanide (n = 10) with the appearance of fast flickering bursts. Second, when the channel did open it spent more time at smaller subconductance levels (Fig. 7*B*). The time course of the experiment is illustrated in Fig. 7*D*. Removing bumetanide from the bath (Fig. 7*C*) produced a full recovery with channel activity showing similar amplitudes and kinetics as in the control condition (Fig. 7*A*). The full recovery required 20–30 sec. Stilbene compounds DIDS and SITS (up to 5 mM) produced no significant effect on channel kinetics (n = 8 for SITS; n = 15 for DIDS) when applied extracellularly. These drugs were not tested in the internal side of the membrane.

Discussion

Selectivity

Although the selectivity sequence, I > Cl > Na > K, indicates that the channel discriminates by charge, the permeability ratios indicate the channel is poorly selective for anions over cations. The sequence was obtained after replacing the E_{rev} in the Goldman-Hodgkin-Katz equation assuming a P_{Na}/P_{Cl} = 0.5 obtained from the E_{rev} with asymmetrical NaCl. However, it is important to mention that this sequence is valid only if the selectivity ratio, P_{Na}/P_{Cl}, remains constant after replacing Na^+ or Cl^- for the cation or anion to be tested.

Anion and Cation-Dependent Permeation

Channel activity was observed only when a combination of a permeable cation and a permeable anion were present on the intracellular side of the membrane. Are there precedents for anion and cation-dependent permeability? An anion channel that is dependent on the presence of a cation has been reported in hippocampal neurons [5]. However, the hippocampal channel is more permeable to Cl^- than the channel we have identified here as demonstrated by a comparison of the magnitude of the shift in reversal potentials in response to alterations in Cl^- concentration gradients. In the neuronal channel the cation facilitates Cl^- permeation; however, the cation itself is poorly permeable [5]. The channel in the T84 cells is half as permeable to Na^+ as Cl^-. Another example of a cation-dependent anion channel is found in molluscan neurons. This anion channel is dependent on the presence of K^+ in the extracellular fluid; however, K^+ ions permeate these channels poorly [6]. Some of the channels that pass both anions and cations rather nonselectively include an ATP-activated skeletal muscle channel [21], the gap junction channel [19] and the human retinal pig-

mental epithelial channel [4]. However, none of these channels has been reported to be dependent on the presence of both permeable anions and cations in order to have a net current movement.

Channel Characteristics

The large conductance of this channel (>200 pS) and the presence of multiple subconductance states are characteristics that resemble those of the family of high conductance voltage-gated anion channels (HVACs) described in a variety of tissues including several epithelial cell lines [11, 12, 15, 18, 22] and nonepithelial cells [1, 2, 6, 16, 17, 20]. The similarities include infrequent occurrence of channel activity in cell-attached patches [2, 11], activation of channels in previously quiescent patches by strong depolarization [15, 16, 18, 22], and relatively poor selectivity between anions and cations [11, 22]. However, there are no reports indicating that these channels are dependent on the presence of permeable anions and cations to be functional. Furthermore, the channel described in the present report showed no voltage sensitivity while the voltage dependence of some of the large conductance anion channels can be described by a Gaussian bell, with the higher *Po* around 0 mV.

Channel Blockers

An interesting feature of this channel is its sensitivity to the loop diuretic bumetanide. Although not quite as sensitive as the $Na^+/K^+/Cl^-$ cotransporter which in most tissues has an IC_{50} between 0.05 μM and 0.5 μM [8] the channel reported here is more sensitive than the KCl transporter [10] and the anion exchanger [7] from red cells. Several anion channels are sensitive to stilbene derivatives (e.g., SITS and DIDS), although this channel was unaffected with SITS or DIDS up to 5 mM.

Multiple Subconductance States

Channel degradation from a 200 pS conductance to multiple subconductance states of 12.5 pS has been described in the anion channel from molluscan neurons [6]. In the present study we have demonstrated that the T84 channel grows from a 15 ± 2 pS conductance to a ≈200 pS conductance. Similarities between the molluscan and the T84 channel are evident. The molluscan channel breaks down into smaller subconductance states, the T84 channel grows to larger amplitudes to reach a maximum level (≈200 pS). This leads to the speculation that an unidentified factor may regulate channel degradation or channel assembly. HVACs such as the T lymphocyte anion channel [17], and the anion channel of the renal-derived epithelial cell line MDCK [11], also appear to be composed of equally sized subconductance states.

An interesting model to explain these results is to consider this channel as a collection of multiple pores, representing the multiple subconductance states. Multi-barreled K^+ channels have been proposed for renal tubule epithelia [13]. A main gating mechanism is thought to operate independently from the subunits (individual pores) which may explain the frequent transitions from any subconductance level to base line, or from base line to the maximum amplitude. An unidentified factor may synchronize the subunits so that the channel open and closes as a unitary conductance. Under certain circumstances, the subunits may operate independently which produces multiple subconductance states. Channel degradation or channel growth may be achieved by partial synchronization.

Channel Function

The function of this channel, as well as that of several other anion channels [11, 15, 18, 22] remains speculative. HVACs from the secretory cell line MDCK appear to be involved in adrenergic-stimulated Cl^- secretion [11]. However, in the bovine kidney epithelial cell line, GBK, substances that increase intracellular cAMP failed to induce channel activity in cell-attached patches containing a similar channel [22]. The latter study is consistent with what we report here. Although channel activation occurred in 25–30% of the patches in response to substances that elevate cAMP in T84 cells or when a permeable form of cAMP was added to the bath, we are not, at the present time, confident that this small percentage actually represents activation by cAMP rather than spontaneous activation. A large conductance anion channel found in T lymphocytes appears to be involved in cell volume regulation [17]. A volume-regulated Cl^- conductance has been described in whole-cell experiments with T84 cells [23]. The role of the channel described in the present report in volume regulation has not yet been assessed.

In conclusion, the channel described here possesses some of the characteristics of the large conductance voltage-gated anion channels (HVACs) described in other tissues. The distinctive characteristics of the T84 channel are lack of voltage dependence in the range ±90 mV, large permeability for Na^+ than most of the HVACs reported thus far

and cation and anion-dependent permeation. The latter has not been reported for other HVACs.

The authors wish to thank Morris Priddy and Charley Roberson for excellent technical assistance and Linda Pai and Steve Valder for participation in the early experiments. This study was supported by UPSH R01-DK39617 to A. Beaudet. L.V. was supported by a one-year fellowship from the Cystic Fibrosis Foundation.

References

1. Blatz, A., Magleby, K. 1989. Single chloride-selective channels active at resting membrane potentials in cultured rat skeletal muscle. *Biophys. J.* **43:**237–241
2. Bosma, M. 1989. Anion channels with multiple conductance levels in a mouse B lymphocyte cell line. *J. Physiol.* **410:**67–90
3. Fabiato, A. 1988. Computer programs for calculating total from specified free or free from specified total ionic concentrations in aqueous solutions containing multiple metals and ligands. *Methods Enzymol.* **157:**378–417
4. Fox, J.A., Pfeffer, B.A., Fain, G.L. 1988. Single channel recordings from cultured retinal human pigment epithelial cells. *J. Gen. Physiol.* **91:**193–222
5. Franciolini, F., Nonner, W. 1987. Anion and cation permeability of a chloride channel in rat hippocampal neurons. *J. Gen. Physiol.* **90:**453–478
6. Geletyuk, V., Kazachenko, V. 1985. Single Cl^- channels in molluscan neurons: multiplicity of the conductance state. *J. Membrane Biol.* **86:**9–15
7. Gunn, R.B. 1985. Bumetanide inhibition of anion exchange in human red blood cells. *Biophys. J.* **47:**326*a*
8. Haas, M. 1989. Properties and diversity of (Na-K-Cl) cotransporters. *Annu. Rev. Physiol.* **51:**443–457
9. Hamill, O., Marty, A., Neher, E., Sakmann, B., Sigworth, F. 1981. Improved patch-clamp techniques for high-resolution current recording from cell and cell-free membrane patches. *Pfluegers Arch.* **391:**85–100
10. Kaji, D. 1986. Volume sensitive K^+ transport in human erythrocytes. *J. Gen. Physiol.* **88:**719–738
11. Kolb, H.A., Brown, C.D.A., Murer, H. 1985. Identification of a voltage-dependent anion channel in the apical membrane of a secretory epithelium (MDCK). *Pfluegers Arch.* **403:**262–265
12. Krouse, M.E., Hagiwara, G., Chen, J., Levinston, N.J., Wine, J.J. 1989. Ion channels in normal human and cystic fibrosis sweat gland cells. *Am. J. Physiol.* **257:**C129–C140
13. Malcolm, H., Giebisch, G. 1987. Multi-barreled K^+ channels in renal tubules. *Nature* **327:**522–524
14. Mandel, K., Dharmathaphorn, K., McRoberts, J.A. 1986. Characterization of a cAMP-activated Cl^- transport pathway in the apical membrane of a human colonic epithelium. *J. Biol. Chem.* **261:**704–712
15. Nelson, D., Tang, J., Palmer, L.J. 1984. Single-channel recordings of apical membrane chloride conductance in A6 epithelial cells. *J. Membrane Biol.* **80:**81–89
16. Nobile, M., Galietta, L. 1988. Large conductance Cl^- channel revealed by patch-recordings in human fibroblasts. *Biochem. Biophys. Res. Comm.* **154:**719–726
17. Schlichter, L., Grygorczyk, R., Pahapill, P., Grygorczyk, C. 1990. A large, multiple-conductance chloride channel in normal human T lymphocytes. *Pfluegers Arch.* **416:** 413–421
18. Schneider, G.T., Cook, D., Gage, P., Young, J. 1985. Voltage-sensitive, high conductance Cl^- channels in the luminal membrane of cultured pulmonary alveolar (type II) cells. *Pfluegers Arch.* **404:**354–357
19. Schwartzmann, G., Wiegandt, H., Rose, B., Zimmerman, A., Ben-Haim, D., Loewenstein, W.R. 1982. Diameter of the cell-to-cell junctional membrane channels as probed with neutral membranes. *Science* **213:**551–553
20. Schwarze, S., Kolb, H. 1984. Voltage-dependent kinetics of an anionic channel of large unit conductance in macrophages and myotube membrane. *Pfluegers Arch.* **402:**281–291
21. Thomas, S.A., Hume, R.I. 1990. Permeation of both cations and anions through a single class of ATP-activated ion channels in developing chick skeletal muscle. *J. Gen. Physiol.* **95:**569–590
22. Velasco, G., Prieto, M., Alvarez-Rivera, J., Gascon, S., Barros, F. 1989. Characteristics and regulation of a high conductance anion channel in GBK kidney epithelial cells. *Pfluegers Arch.* **414:**304–310
23. Worrel, R.T., Butt, A.G., Cliff, W.H., Frizzell, R.A. 1989. A volume-sensitive chloride conductance in human colonic cell line T84. *Am. J. Physiol.* **256:**C1111–C1119

Received 2 February 1992; revised 26 May 1992